N-cadherin–mediated cell adhesion restricts cell proliferation in the dorsal neural tube

Kavita Chalasani* and Rachel M. Brewster
Department of Biological Sciences, University of Maryland Baltimore County, Baltimore, MD 21250

ABSTRACT **Neural progenitors are organized as a pseudostratified epithelium held together by adherens junctions (AJs), multiprotein complexes composed of cadherins and α- and β-catenin. Catenins are known to control neural progenitor division; however, it is not known whether they function in this capacity as cadherin binding partners, as there is little evidence that cadherins themselves regulate neural proliferation. We show here that zebrafish N-cadherin (N-cad) restricts cell proliferation in the dorsal region of the neural tube by regulating cell-cycle length. We further reveal that N-cad couples cell-cycle exit and differentiation, as a fraction of neurons are mitotic in *N-cad* mutants. Enhanced proliferation in *N-cad* mutants is mediated by ligand-independent activation of Hedgehog (Hh) signaling, possibly caused by defective ciliogenesis. Furthermore, depletion of Hh signaling results in the loss of junctional markers. We therefore propose that N-cad restricts the response of dorsal neural progenitors to Hh and that Hh signaling limits the range of its own activity by promoting AJ assembly. Taken together, these observations emphasize a key role for N-cad–mediated adhesion in controlling neural progenitor proliferation. In addition, these findings are the first to demonstrate a requirement for cadherins in synchronizing cell-cycle exit and differentiation and a reciprocal interaction between AJs and Hh signaling.**

Monitoring Editor
Alpha Yap
University of Queensland

Received: Aug 6, 2010
Revised: Feb 18, 2011
Accepted: Feb 24, 2011

INTRODUCTION

Adherens junctions (AJs) are multiprotein complexes that include classical cadherins, the adhesive component of the AJ, and α-catenin (α-cat) and β-catenin (β-cat). β-cat binds to the cadherin cytoplasmic domain and provides a connection to the actin cytoskeleton by interacting dynamically with α-cat (Nelson, 2008). In addition to mediating cell–cell adhesion, AJs are required for the establishment of apicobasal polarity because they set up spatial cues for signaling complexes that enable apical domain formation (Niessen and Gottardi, 2008). Thus deletion of any of the core components of AJs results in loss of both cell–cell adhesion and polarity (Niessen and Gottardi, 2008). Cadherins and catenins are also known to influence cell proliferation during embryonic development and cancer progression (Vasioukhin *et al.*, 2001; Machon *et al.*, 2003; Zechner *et al.*, 2003; Kobielak and Fuchs, 2006; Perrais *et al.*, 2007; Benjamin and Nelson, 2008; Grigoryan *et al.*, 2008; Jeanes *et al.*, 2008); however, it remains controversial whether these proteins function together (in the context of AJs) or independently of one another, as they are known to associate with multiple signaling partners (Clevers, 2006; Scott and Yap, 2006; Benjamin and Nelson, 2008; Jeanes *et al.*, 2008; Lien *et al.*, 2008b). For example, E-cadherin can inhibit or modulate growth factor signaling through its functional interaction with the epidermal growth factor receptor (Jeanes *et al.*, 2008). β-cat functions as the downstream effector of the Wnt signaling pathway, in addition to being an AJ component (Clevers, 2006). Increasing evidence also suggests that α-cat regulates proliferation, trafficking, and actin dynamics independently of cadherins (Scott and Yap, 2006; Benjamin and Nelson, 2008; Lien *et al.*, 2008a, 2008b; Tinkle *et al.*, 2008; Benjamin *et al.*, 2010). As with other aspects of cadherin-based adhesion, the mechanisms by which cadherins and catenins control cell proliferation are likely to be context-specific.

In the neural tube, deletion of β-cat results in withdrawal of progenitors from the cell cycle (Machon *et al.*, 2003; Zechner *et al.*,

This article was published online ahead of print in MBoC in Press (http://www.molbiolcell.org/cgi/doi/10.1091/mbc.E10-08-0675) on March 9, 2011.

*Present address: Department of Otolaryngology–Head & Neck Surgery, Stanford University School of Medicine, Stanford, CA 94305–5739.

Address correspondence to: Rachel M. Brewster (brewster@umbc.edu).

Abbreviations used: α-cat, α-catenin; Ace-Tub, acetylated-tubulin; AJs, adherens junctions; aPKC, atypical PKC; β-cat, β-catenin; BrdU, bromodeoxyuridine; ETOH, ethyl alcohol; Hh, Hedgehog; hpf, hours postfertilization; MO, morpholino; N-cad N-cadherin; PFA, paraformaldehyde; PH3, phospho histone3; *ptc1*, *patched1*; *shh*, *sonic hedgehog*; Smo, Smoothened; som, somites; *twhh*, *tiggywinkle hedgehog*.

© 2011 Chalasani and Brewster. This article is distributed by The American Society for Cell Biology under license from the author(s). Two months after publication it is available to the public under an Attribution–Noncommercial–Share Alike 3.0 Unported Creative Commons License (http://creativecommons.org/licenses/by-nc-sa/3.0).

"ASCB®," "The American Society for Cell Biology®," and "Molecular Biology of the Cell®" are registered trademarks of The American Society of Cell Biology.

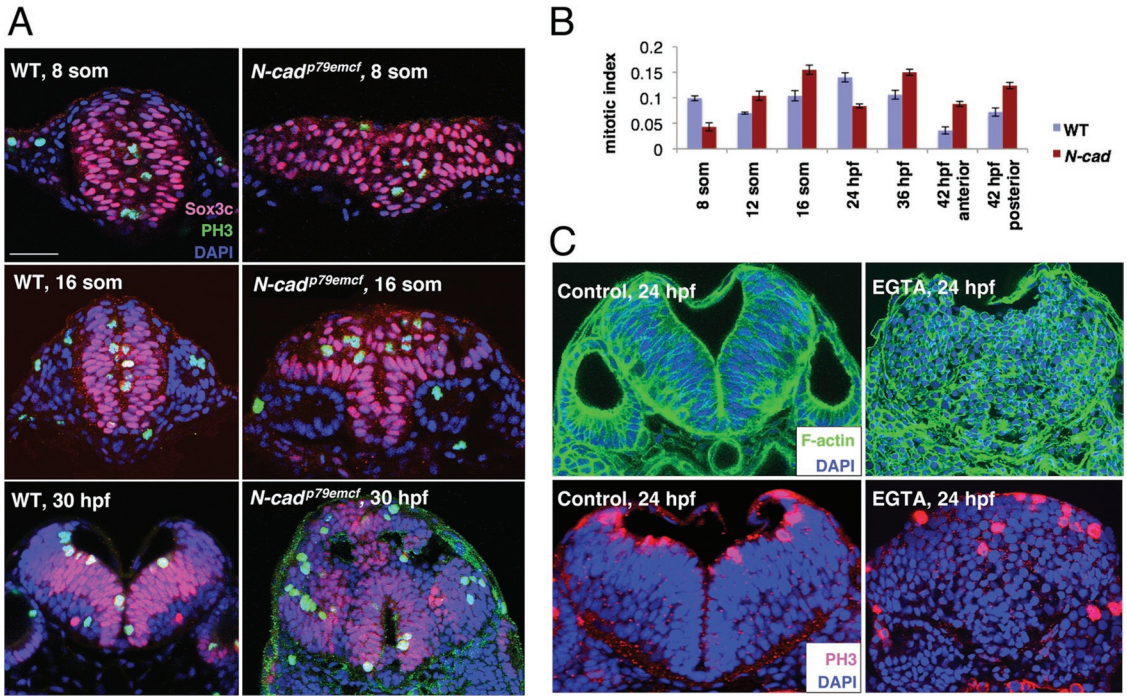

FIGURE 1: Cell proliferation is increased in *N-cad* mutants. All panels in this figure and subsequent figures show representative images of cross-sections through the hindbrain region of the indicated genotype. Images are oriented dorsal to the top. (A) WT and *N-cad*^{p79emcf} embryos labeled with anti-Sox3C (neural progenitor marker, pink), anti-PH3 (mitotic marker, green), and DAPI (nuclear marker, blue) at 8 som, 16 som, and 30 hpf. (B) Quantification of mitotic indices in WT and *N-cad*^{p79emcf} mutants at different stages of development. Mitotic indices were quantified as the ratio of mitotic cells (PH3-positive) to the total number of progenitors (Sox3C-positive). Statistical significance was assessed using the logistic regression analysis (SAS system), and p values are 0.002 (8 som), 0.003 (12 som), 0.0001 (16 som), 0.0001 (24 hpf), 0.03 (36 hpf), 0.0042 (42 hpf anterior), and 0.021 (42 hpf posterior). (C) Untreated control and EGTA-treated embryos labeled with phalloidin and anti-PH3. Scale bar = 20 μm.

2003), whereas overexpression of a stable form of β-cat triggers expansion of the precursor population (Chenn and Walsh, 2002). In contrast, it is deletion of α-E-cat in neural progenitors that causes brain hyperplasia. The latter phenotype is mediated by up-regulation of Hedgehog (Hh) signaling, although the underlying mechanism is not well understood (Lien *et al.*, 2006). While the α-E-cat phenotype is consistent with a role for AJs in regulating proliferation in the brain, there is a lack of evidence that cadherins themselves are implicated in the control of cell division. A conditional knockout of *N-cad*, a member of the classical cadherin subfamily expressed prominently in the neural tissue (Hatta and Takeichi, 1986; Radice *et al.*, 1997; Harrington *et al.*, 2007), revealed that internal structures of the cerebral cortex are disorganized, but a cell proliferation defect was not reported in these mice (Kadowaki *et al.*, 2007). In *KIF3* mouse knockouts, in which N-cad localization is abnormal, enhanced proliferation of neural progenitor cells is observed (Teng *et al.*, 2005); however, this evidence is indirect as kinesin is required for the proper localization of multiple proteins. In zebrafish *N-cad* mutants, cell proliferation is enhanced in the hindbrain region, although this increase was reported to be transient (Lele *et al.*, 2002). We reinvestigate here the role of zebrafish *N-cad* in controlling cell proliferation in the neural tube and reveal striking similarities with the α-E-cat loss-of-function phenotype.

RESULTS

Dorsal neural progenitors hyperproliferate in *N-cad* mutants

To gain further insight into the role of zebrafish *N-cad*, we quantified mitotic indices in the hindbrain of *N-cad*^{p79emcf} mutants and observed an increase in the mitotic index at the 12–13 somites (som) stage that was sustained at later developmental stages (Figure 1, A and B), with the exception of 24 h postfertilization (hpf) when it is in fact slightly reduced (0.7-fold). This reduction may be the consequence of early symmetric divisions (Lyons *et al.*, 2003), producing mitotic progenitors rather than postmitotic neurons and resulting in a 1.6-fold increase in the total cell number by 24 hpf (Supplemental Figure S1). An increase in cell division is also observed in *N-cad*^{tR210} mutants, *N-cad* morpholino (MO)-injected embryos (unpublished data), and EGTA (disruptor of calcium-dependent cell–cell adhesion)–treated embryos (Figure 1C). These findings confirm that the increase in cell division in *N-cad* mutants occurs at the 12–13 som stage, as previously reported (Lele *et al.*, 2002); however, we demonstrate that enhanced cell division is sustained at later stages of development.

In the zebrafish neural tube, N-cad is distributed throughout the plasma membrane during neurulation and becomes enriched in AJs upon neural tube closure (Geldmacher-Voss *et al.*, 2003; Hong and Brewster, 2006). This dynamic shift in localization raises the question of whether N-cad regulates cell proliferation as an AJ component. In support of this model, the developmental stage (12–13 som) at which the increase in mitosis is first observed coincides with the onset of AJ formation in wild-type (WT) embryos (Geldmacher-Voss *et al.*, 2003; Hong and Brewster, 2006). To further investigate a connection with AJs, we quantified the percentage of mitotic cells in dorsal versus ventral regions of the neural tube, as it was previously shown that AJs are absent only in dorsal regions of *N-cad* mutants (Lele *et al.*, 2002; Hong and Brewster, 2006). We found that the

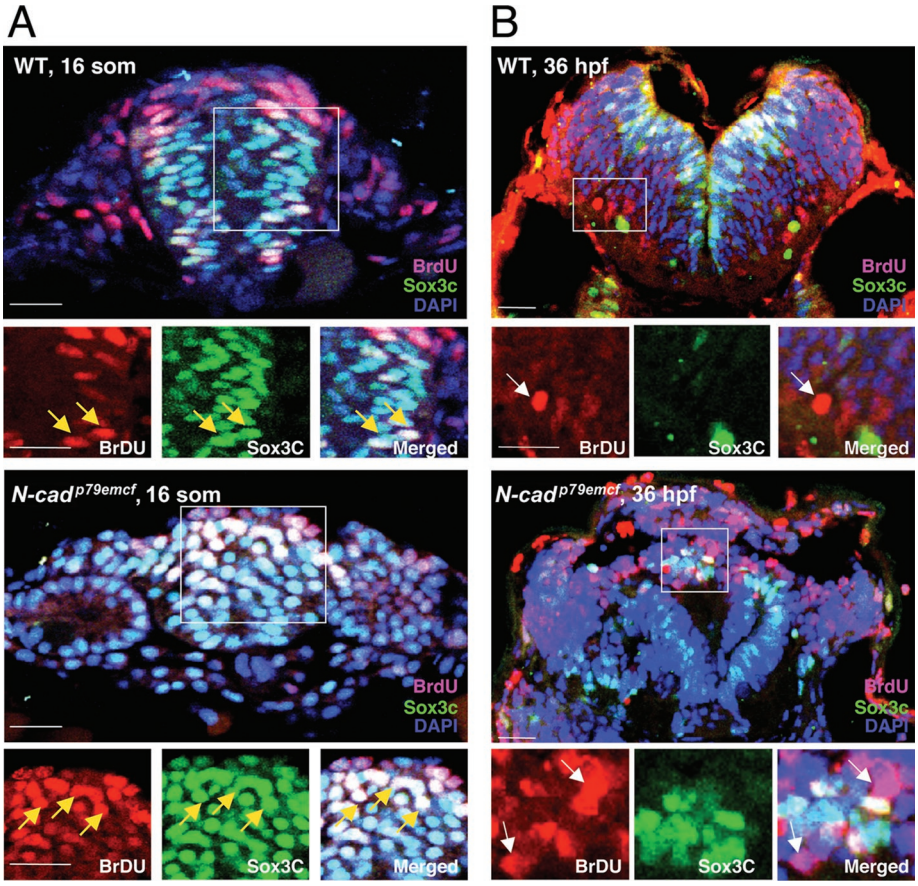

FIGURE 2: Cell-cycle length but not cell-cycle exit is decreased in *N-cad* mutants. (A) WT and *N-cad*^{p79emcf} embryos were exposed to a short pulse of BrdU at 16 som and labeled with anti-BrdU (red), anti-Sox3C (green), and DAPI (blue). The boxes indicate area shown in single channels in bottom panels. Yellow arrows point to mitotic progenitors. (B) WT and *N-cad*^{p79emcf} embryos exposed to a short pulse of BrdU at 12 som, fixed at 36 hpf, and labeled with anti-BrdU (red), anti-Sox3C (green), and DAPI (blue). Boxes indicate the area that was magnified 2.6-fold in bottom panels. White arrows point to BrdU-positive cells that have exited the cell cycle. Scale bar = 20 μm.

increase in mitosis is indeed highest in dorsal regions (71% of all mitotic cells in *N-cad* mutants are dorsally restricted at 12 som). Surprisingly, hyperproliferation is also dorsally restricted in EGTA-treated embryos in which AJs are disrupted throughout the entire neural tube (Figure 1C). These observations suggest that N-cad is likely to function as an AJ component in repressing cell proliferation, but this function is confined to dorsal regions.

Cell-cycle length is shortened in *N-cad* mutants

At the cellular level, increase in cell proliferation is typically caused by a decrease in cell-cycle exit or by a shortening of cell-cycle length. To determine whether cell-cycle length is reduced in *N-cad*^{p79emcf} mutants, we scored, in 36 hpf embryos, the ratio of Sox3C (a neural progenitor marker)–positive cells labeled by a pulse of bromodeoxyuridine (BrdU). If the cell cycle is shortened, then there is a higher probability that progenitors would be in the S phase of the cell cycle and thus labeled with BrdU. Therefore the ratio of Sox3C-BrdU double-positive cells to the total number of Sox3C-positive cells would be higher for mutants than for WT. We indeed observed a significant increase in the ratio of these double-positive cells in *N-cad*^{p79emcf} mutants beginning at the 14 som stage (0.318 in WT and 0.424 in *N-cad* mutants, p = 0.00037) and extending to 16 som (Figure 2A).

To determine whether cell-cycle exit may also be altered in *N-cad*^{p79emcf} mutants, we exposed embryos to a pulse of BrdU at 12 som and scored the percentage of BrdU-positive cells that exited the cell cycle, and hence were either Sox3C-negative or HuC-positive (HuC is a neuronal marker; Pascale *et al.*, 2008), by 36 hpf. We reasoned that a decrease in cell-cycle exit would result in a lower fraction of BrdU-positive and Sox3C-negative or BrdU-positive and HuC-positive cells in the hindbrain region. We found no difference in cell-cycle withdrawal between WT and *N-cad*^{p79emcf} mutants labeled with BrdU and anti-Sox3C (Figure 2B; 96.8% for mutants vs. 92.6% for WT, p = 0.07) or with BrdU and anti-HuC (unpublished data). These findings indicate that cell-cycle length rather than cell-cycle exit is altered in *N-cad* mutants.

Cell-cycle exit and differentiation appear uncoupled in *N-cad* mutants

Although differentiation is not impaired, we and others have shown that the distribution of neurons and mitotic, Phospho Histone3 (PH3)-positive, cells in the hindbrain is abnormal in *N-cad* mutants, as differentiated cells are found adjacent to mitotic precursors (Kadowaki *et al.*, 2007; Chalasani and Brewster, 2010). Interestingly, further analysis of embryos double-labeled with anti-PH3 and anti-HuC or the HuC-Kaede transgene (Sato *et al.*, 2006) revealed that a small but significant percentage of cells coexpressed both markers in *N-cad*^{p79emcf} mutants or MO-injected embryos (Figure 3, A and C). Since this observation contradicts the commonly held view that cells need to exit the cell cycle to differentiate (Buttitta and Edgar, 2007), we investigated whether mitotic cells that are HuC-positive express other markers indicative of neuronal differentiation. We immunolabeled 48 hpf embryos from the HuC-Kaede transgenic line with anti-PH3 and anti-Acetylated-Tubulin (Ace-Tub; an axonal microtubule marker) and observed that many HuC-positive mitotic cells in *N-cad*^{p79emcf} mutants appear to extend axonal processes (Figure 3B). These observations suggest that cadherins are required to couple cell-cycle exit and differentiation in the neural tube. The presence of mitotic, HuC-positive neurons does not contradict the finding that cell-cycle withdrawal appears normal in 36 hpf mutants. Indeed, it is unclear whether cell-cycle withdrawal is normal at 48 hpf when most mitotic neurons are observed. Furthermore, mitotic neurons represent such a small fraction of the total number of dividing cells (7% of all PH3-positive cells at 48 hpf) that their presence is unlikely to cause a noticeable change in the rate of cell-cycle withdrawal, irrespective of the developmental stage at which the cell cycle was analyzed.

Hyperproliferation in *N-cad* mutants is mediated by Hh signaling

Hyperproliferation in *N-cad* mutants is likely to be caused by deregulation of a signaling pathway that promotes neural progenitor division. A likely candidate pathway is canonical Wnt signaling that

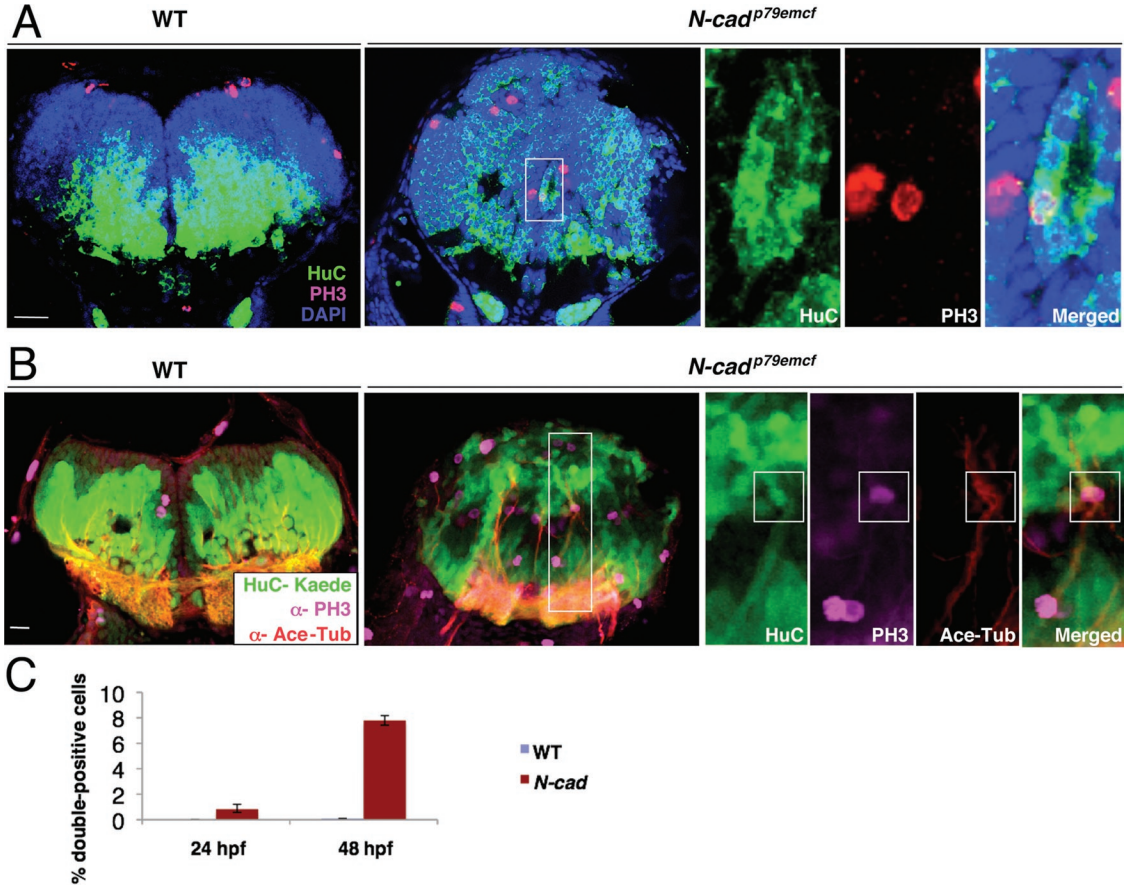

FIGURE 3: Cell-cycle exit and differentiation are uncoupled in *N-cad* mutants. (A) WT and *N-cad*^{p79emcf} embryos at 48 hpf labeled with anti-HuC (neuronal marker, green), anti-PH3 (pink), and DAPI (blue). The box indicates the region that was magnified 2.3-fold in panels to the right, in which single and merged channels are shown. (B) HuC-Kaede (green) transgenic WT and *N-cad*^{p79emcf} mutants labeled with anti-PH3 (pink) and anti-Ace-Tub (axonal marker, red). The box indicates the region that was magnified 2.4-fold in panels to the right, in which single and merged channels are shown. (C) Percentage of mitotic cells in the hindbrain of WT and *N-cad*^{p79emcf} mutants at 24 hpf and 48 hpf that are double-positive for PH3 and HuC. Scale bar = 20 μm.

has been shown to regulate cell proliferation in the brain (Chenn and Walsh, 2002; Megason and McMahon, 2002; Machon *et al.*, 2003; Zechner *et al.*, 2003; Panhuysen *et al.*, 2004; Alvarez-Medina *et al.*, 2009), most likely through transcriptional control of *cyclin-D1* (Shtutman *et al.*, 1999), a regulator of the G1/S phase of the cell cycle. Classical cadherins can act as a "sink" for Wnt/β-cat signaling by sequestering β-cat at the membrane, away from this signaling pathway (Jeanes *et al.*, 2008). To address whether Wnt signaling is enhanced in dorsal regions of the neural tube in *N-cad* mutants, we analyzed the expression of two Wnt downstream targets, *cyclin-D1* and *axin2*, but we did not observe overexpression of either of these markers in the neural tube (unpublished data).

We next investigated whether ectopic Hh signaling may underlie hyperproliferation in *N-cad* mutants, as several studies have reported that Hh promotes neural progenitor division (Jeong and McMahon, 2005; Cayuso *et al.*, 2006; Locker *et al.*, 2006; Alvarez-Medina *et al.*, 2009). Furthermore, disruption of α-E-cat causes hyperproliferation in the mouse brain, mediated by the Hh pathway (Lien *et al.*, 2006). To determine whether Hh signaling is up-regulated in *N-cad* mutants, we analyzed mRNA expression of *sonic hedgehog (shh)* and downstream signaling components *patched1 (ptc1), gli1, and gli2a* in 16 som WT and *Ncad* MO-injected embryos. *ptc1* and *gli1* are transcriptional targets of Hh signaling (Chen and Struhl, 1996; Lee *et al.*, 1997) in addition to being mediators of this pathway. We observed an expansion of *ptc1* and *gli1* expression in dorsal regions of the neural tube in N-cad–depleted embryos compared with controls (Figure 4A, circled areas). The expanded area of *ptc1* and *gli1* expression correlates with the region in which we observe increased cell division in *N-cad* mutants (Figure 1A). In contrast, *shh* and *gli2* RNA expression is unchanged, suggesting that it is the range of Hh signaling that it is expanded. To test whether up-regulation of Hh signaling may be the cause for hyperproliferation in *N-cad* mutants, we blocked Smoothened (Smo), the membrane protein that mediates Hh signaling, using the drug cyclopamine (Chen *et al.*, 2002) and scored mitotic indices in WT and *N-cad*$^{R2.10}$ mutants (Figure 4, B and C). We found that treatment of WT embryos with cyclopamine had no effect on mitotic indices (Figure 4C), indicating that Hh does not promote cell proliferation, at least at 16 som. In contrast, treatment of *N-cad*$^{R2.10}$ mutants with cyclopamine effectively reduced hyperproliferation (Figure 4C). A reduction in hyperproliferation was also observed in *N-cad*$^{R2.10}$ mutants that received injections of *gli1* and *gli2* MOs, confirming that expanded Hh signaling is the underlying cause for enhanced cell division in *N-cad* mutants (Figure 5, A and B).

Dorsal expansion of Hh signaling in N-cad–depleted embryos could be explained by broader ligand diffusion, due to loss of cell–cell adhesion (Lele *et al.*, 2002), or by a ligand-independent activation of the pathway. To distinguish between these possibilities, we

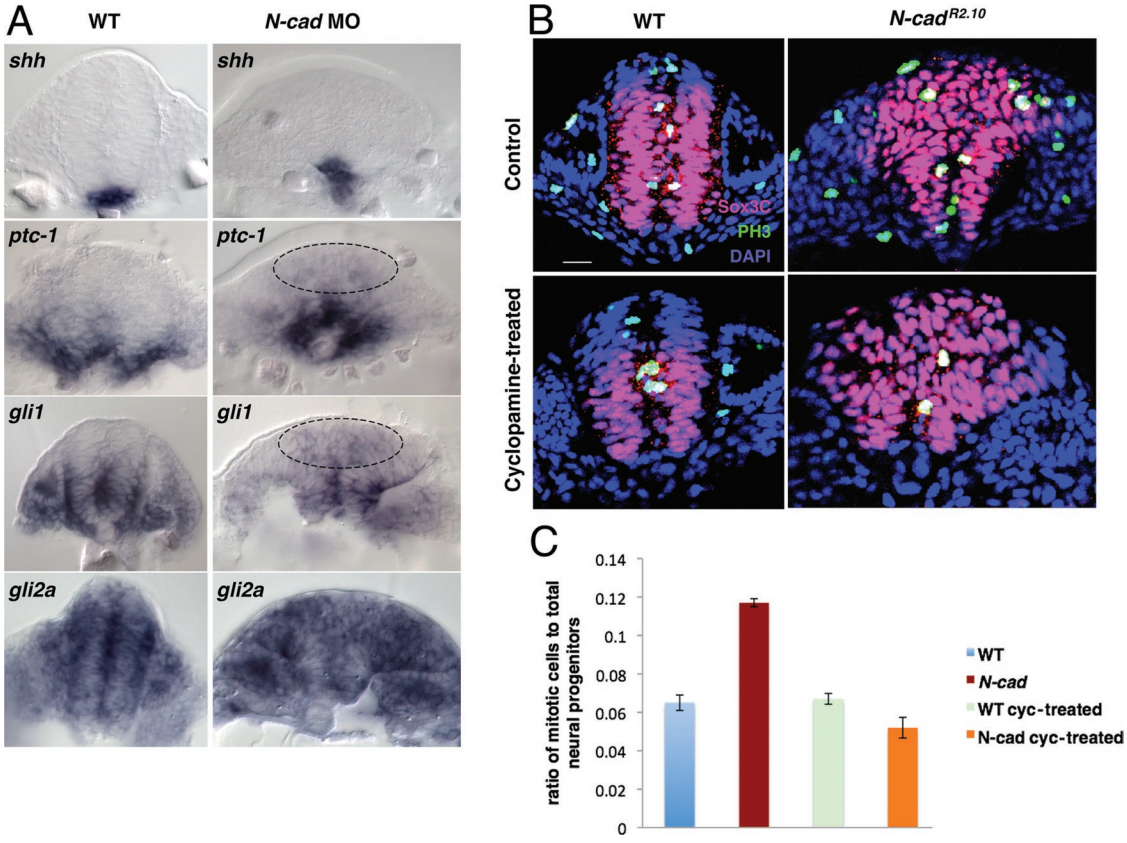

FIGURE 4: Hyperproliferation in *N-cad* mutants is mediated by Hh signaling. (A) Control and *N-cad* MO-injected embryos labeled by in situ hybridization with *shh, ptc-1, gli1,* and *gli2a* riboprobes at 16 som. Dorsal ectopic expression of *ptc-1* and *gli1* in *N-cad* MO-injected embryos is indicated by dashed circles. Scale bar = 10 µm. (B) WT and *N-cad*$^{R2.10}$ controls and cyclopamine-treated embryos, labeled with anti-Sox3C (pink), anti-PH3 (green), and DAPI (blue). Scale bar = 20 µm. (C) Mitotic indices in WT and *N-cad*$^{R2.10}$ embryos treated with cyclopamine. Indices were quantified as the ratio between mitotic cells and total number of progenitors. Statistical significance was assessed using Student's *t* test; p = 0.0047 between WT and *N-cad* controls; p = 0.0066 between *N-cad* control and cyclopamine-treated embryos.

tested whether MO depletion of *shh* and *tiggywinkle hedgehog (twhh)* in *N-cad*$^{R2.10}$ mutants can prevent hyperproliferation. We found that the mitotic indices for control (uninjected) *N-cad*$^{R2.10}$ mutants are similar to the values for *shh/twhh* MO-depleted *N-cad*$^{R2.10}$ mutants and that both values are significantly higher than those for WT controls (Figure 5, A and B), indicating that rescue did not take place. In contrast, blocking Hh signaling downstream of the ligand (using *gli1/gli2* MOs) rescues the hyperproliferation phenotype (Figure 5, A and B). Together, these findings suggest that Smo is either activated independently of Hh or transduces the Hh signal more effectively in N-cad–depleted embryos.

We next asked whether defective cilia could account for ligand-independent activation of Hh signaling in *N-cad* mutants, as cilia are essential processing sites for Hh signal transduction in vertebrates (Eggenschwiler and Anderson, 2007; Huang and Schier, 2009; Kim *et al.*, 2010; Wilson and Stainier, 2010). To image cilia, we immunolabeled 16 som embryos with anti-Ace-Tub (a cilia marker also associated with axons) and anti-γ-Tub (a basal body marker). We observed that, in *N-cad*$^{R2.10}$ mutants, these organelles are present; however, they are 0.7-fold shorter than in WT embryos (Figure 6, A and B). Defective ciliogenesis in zebrafish *iguana* mutants is linked to improper Hh signaling (Kim *et al.*, 2010; Wilson and Stainier, 2010). Furthermore, ligand independent, constitutive activation of low levels of Gli activators has been reported in *arl13b* mutant mice in which cilia length is reduced (Caspary *et al.*, 2007). It is therefore possible that the cilia defects in *N-cad* mutants contribute to increased Hh signaling and proliferation in these embryos.

Because enhanced Hh signaling appears to underlie hyperproliferation in *N-cad* mutants, we next tested whether overexpression of *shh* mRNA is sufficient to cause hyperproliferation of neural progenitors in the zebrafish embryo. We observed a twofold increase in the mitotic index of 16 som *shh* injected versus control embryos (0.069 for controls vs. 0.15 for injected, n = 5 embryos, p = 0.0002), confirming a promitotic role for *shh* (Figure 7, A and B). We also investigated whether *shh* is responsible for uncoupling cell-cycle exit and differentiation in *N-cad* mutants, by scoring *shh*-injected embryos for the presence of mitotic neurons. In contrast to *N-cad* mutants (Figure 3A), PH3 and HuC double-positive cells were not observed in *shh*-injected embryos (unpublished data), suggesting a different signaling mechanism.

Hh signaling promotes AJ assembly

The ectopic expression of Hh pathway targets in *N-cad* mutants and the rescue of hyperproliferation observed in embryos impaired in Hh signaling suggest that this pathway is regulated downstream of AJs. However, it has been reported that *shh* promotes cell adhesion in the mouse neural tube (Jarov *et al.*, 2003; Fournier-Thibault *et al.*, 2009), suggesting that the interaction between cell adhesion/polarity

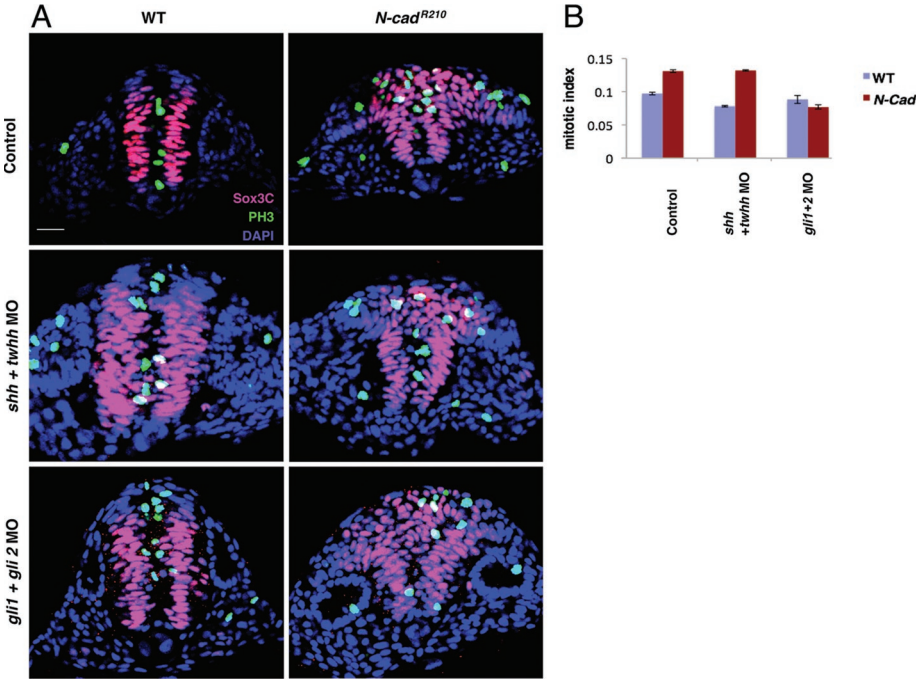

FIGURE 5: Hyperactivation of Hh signaling in *N-cad* mutants occurs downstream of Hh ligands. (A) WT and *N-cad*$^{R2.10}$ controls, *shh/twhh* MO-injected and *gli1/gli2* MO-injected embryos, at 16 som labeled with anti-Sox3C (pink), anti-PH3 (green), and DAPI (blue). Scale bar = 20 μm. (B) Mitotic indices in WT and *N-cad*$^{R2.10}$ uninjected controls, and embryos injected with *shh/twhh* MO or *gli1/gli2* MO. Indices were quantified as the ratio between mitotic cells and the total number of progenitors. Statistical significance was assessed using a Student's *t* test; p = 0.001 between WT and *N-cad* mutant; p = 0.8 between *N-cad* mutant and *N-cad* shh/twhh MO-injected embryos; p = 0.0001 between *N-cad* control and *N-cad gli1/gli2* MO-injected embryos.

regulators and the Hh pathway may not be strictly linear. To determine whether Hh signaling regulates the assembly or localization of junctional complexes in the zebrafish neural tube, we analyzed the expression of junctional markers F-actin (a marker for cortical actin enriched in AJs), Z0–1 (a tight junction marker), and atypical protein kinase C (aPKC) (an apical marker) in WT embryos exposed to cyclopamine. In 16 som control-untreated embryos, these markers are localized along the midline of the neural tube where AJs form, indicative of apicobasal polarity. In contrast, these markers appear discontinuous in dorsal regions of cyclopamine-treated embryos (Figure 8A; n = 3 of 4 embryos). At 36 hpf, apical markers remain reduced in cyclopamine-treated embryos (Figure 8B; n = 5 of 5 embryos), suggesting that there is a blockage rather than a delay in cell polarization. In addition, the neural tube is significantly smaller than that of untreated controls, possibly as a consequence of decreased cell proliferation (occurring after 16 som) and/or apoptosis. To confirm the lack of polarization in cyclopamine-treated embryos, we analyzed other hallmarks of apicobasal polarity in the zebrafish neural tube, namely, the ability of nuclei to align on either side of the midline at the neural rod stage (asterisks in Figure 8A) and the presence of a neurocoele at 36 hpf (asterisks in Figure 8B; Munson *et al.*, 2008). Analysis of these markers in cyclopamine-treated embryos revealed that nuclei straddle the dorsal midline at 16 som (arrowhead in Figure 8A; n = 4 of 4 embryos) and that the neurocoele is absent at 36 hpf (Figure 8B; n = 5 of 5 embryos). The cell adhesion/polarity defects observed in cyclopamine-treated embryos are overall similar to those reported for *pard6γb* mutants in which apicobasal polarity is disrupted (Munson *et al.*, 2008). These findings reveal that disruption of Hh signaling prevents junctional complex assembly and apicobasal polarity in dorsal regions of the neural tube, indicating that the rescue of proliferation defects in *N-cad* mutants depleted for Hh signaling occurs despite proper polarization. Since all apical markers tested are reduced in cyclopamine-treated embryos, Hh is likely to control an early event in cell polarization, possibly the assembly of AJs (Niessen and Gottardi, 2008).

DISCUSSION

We demonstrate here that loss of N-cad function in zebrafish embryos results in hyperproliferation in the dorsal region of the neural tube, mediated by ectopic Hh signaling. These findings suggest that N-cad is normally required to restrict the proliferation of dorsal progenitors, thereby maintaining a steady state of division in the neural tube. Hyperproliferation in *N-cad* mutants appears to be caused by a loss of AJs, as the onset of the phenotype coincides with the timing when these junctional complexes are normally assembled in WT embryos. In addition, the region where AJs are disrupted overlaps with the area where enhanced cell proliferation is observed.

Several studies have demonstrated that α-cat (Lien *et al.*, 2006) and β-cat (Chenn and Walsh, 2002; Machon *et al.*, 2003; Zechner *et al.*, 2003) also regulate cell proliferation in the brain. These catenins are known to have cadherin-independent roles in signaling, raising the question of whether they function in the context of AJs to control cell-cycle progression. It is possible, for instance, that catenins function strictly in an adhesion-independent manner to regulate the cell cycle. In this scenario, the hyperproliferation observed in *N-cad* mutants may merely be caused by a change in the subcellular distribution of one of these proteins (due to disruption of AJs), which in turn activates a catenin-mediated signaling event (Jeanes *et al.*, 2008; Lien *et al.*, 2008b). However, we provide several pieces of evidence suggesting that cadherin-dependent properties of catenins are indeed required, at least in part, to restrict cell proliferation in the brain. With regard to β-cat–mediated signaling, we have found that Wnt downstream targets, *cyclin-D1* and *axin2*, are not up-regulated in *N-cad* mutants. As for α-E-cat, its loss rather than gain of function causes hyperproliferation (Lien *et al.*, 2006), arguing against deregulation of α-cat–mediated signaling as the underlying cause for enhanced division in *N-cad* mutants.

Disruption of AJs in *N-cad* mutants results in a substantial loss of cell–cell adhesion and apicobasal polarity in the neural tube. It is therefore possible that a general perturbation in tissue integrity contributes to hyperproliferation in *N-cad* mutants. The loss-of-function phenotype of the cell polarity regulator Lgl1 argues against this possibility, however. Tissue integrity is also severely compromised in *lgl1* mutants but it is deregulation of Notch rather than Hh signaling that is thought to contribute to hyperproliferation in these embryos (Vasioukhin, 2006). The specificity of the *lgl1* and *N-cad* loss-of-function phenotypes suggests that cell polarity regulators interact with specific signaling pathways implicated in cell-cycle control and consequently that their loss of function causes hyperproliferation for different reasons. Another piece of evidence suggesting that impaired tissue integrity is not the

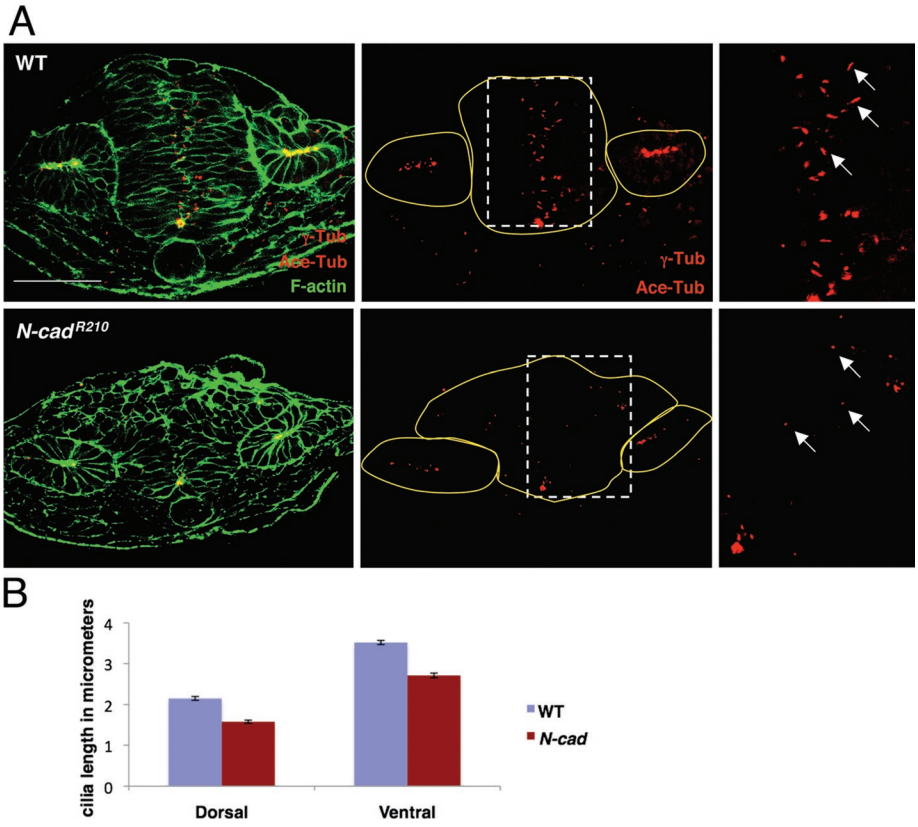

FIGURE 6: N-cad is required for ciliogenesis. (A) Sections of WT and *N-cad*$^{R2.10}$ embryos at 16 som labeled with anti-γ-Tub (basal body marker, red), anti-Ace-Tub (cilia marker, red), and phalloidin (green). The box indicates the region that was magnified twofold in panels to the right. The yellow line delineates the shape of the neural tube and otic vesicles. Arrows indicate individual cilia. Scale bar = 20 μm. (B) Quantification of cilia length in WT and *N-cad*$^{R2.10}$ embryos at 16 som, in dorsal and ventral regions. Statistical significance was assessed using the logistic regression analysis (SAS system), p = 0.0007 for dorsal and p = 0.001 for ventral regions.

underlying cause for enhanced proliferation in *N-cad* mutants stems from the fact that EGTA treatment, which disrupts adhesion throughout the neural tube, causes enhanced proliferation in the dorsal region of neural tube only (Figure 1C).

N-cad's role in regulating growth of the neural tube is likely to involve more than control of cell-cycle progression, because we also observe an uncoupling of cell-cycle exit and differentiation in *N-cad* mutants. Unlike the increase in cell proliferation in *N-cad* mutants, Hh signaling does not influence the ability of neurons to divide, indicating a Hh-independent role of N-cad in this context. The fact that mitotic neurons are mostly observed at late stages of development in *N-Cad* mutants (48 hpf) suggests that there is a temporal requirement for N-Cad in coupling cell-cycle exit and differentiation. Another explanation for the late onset of the mitotic neurons phenotype is that N-cad may prevent reentry of neurons into the cell cycle rather than promoting cell differentiation upon cell cycle exit. In this alternative scenario, neural progenitors that exited the cell cycle normally at 36 hpf may be able to reenter the cell cycle at 48 hpf in the absence of N-Cad function. Regardless of the mechanism, the fact that mitotic neurons are observed in *N-cad* mutants adds to the growing evidence that withdrawal of neural progenitors from the cell cycle and differentiation may in fact be separable events in the nervous system (Firth and Baker, 2005; Sage *et al.*, 2005; Buttitta *et al.*, 2007, 2010) that happen to be controlled by the same molecules (Sellers *et al.*, 1998; Buttitta and Edgar, 2007; Chen *et al.*, 2007).

Misexpression of Hh targets in *N-cad* and α-*E-cat* mutants suggests that AJs normally restrict the activity of the Hh pathway in dorsal regions of the neural tube. The exact role of N-cad in this process is likely to be indirect, as cadherins themselves do not function as signaling molecules. We demonstrate that the molecular mechanism underlying ectopic activation of Hh signaling in *N-cad* mutants is ligand-independent, because blockage of Smo with cyclopamine or treatment with *gli1* and *gli2* MO rescues the hyperproliferation phenotype in *N-cad* mutants, but depletion of Twhh and Shh does not. We further speculate that deregulation of the Hh pathway in *N-cad* mutants may be linked to abnormal cilia, organelles known to function as important processing centers for Hh signaling in mammals (Eggenschwiler and Anderson, 2007) as well as zebrafish (Huang and Schier, 2009; Kim *et al.*, 2010; Wilson and Stainier, 2010). The number and growth of these organelles is strikingly reduced in both dorsal and ventral regions of the neural tube in *N-cad* mutants. This study is the first, to our knowledge, to establish a link between classical cadherins and ciliogenesis. Other members of the cadherin superfamily, Celsr2 and Celsr3 (Flamingo homologues), are required for ependymal cilia growth (Tissir *et al.*, 2010). It will therefore be interesting to determine in the future whether different members of the cadherin family function together to promote ciliogenesis.

Early studies have demonstrated that Shh promotes ventral cell fates in the neural tube (Ericson *et al.*, 1997). Several more recent articles indicate that Shh signaling also

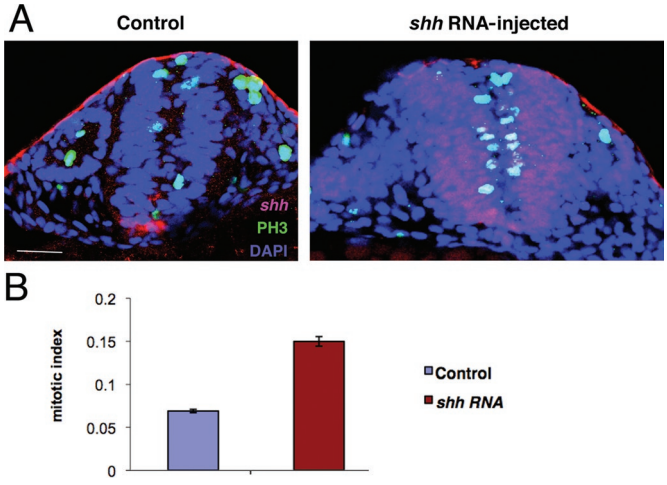

FIGURE 7: Overexpression of *shh* results in hyperproliferation. (A) Control and *shh* RNA-injected embryos at 16 som labeled with *shh* (red), anti-PH3 (green), and DAPI (blue). Scale bar = 20 μm. (B) Mitotic indices in control and *shh* RNA-injected embryos. Indices were quantified as the ratio between mitotic cells and the total number of cells. Statistical significance was assessed using a Student's *t* test, p = 0.0002.

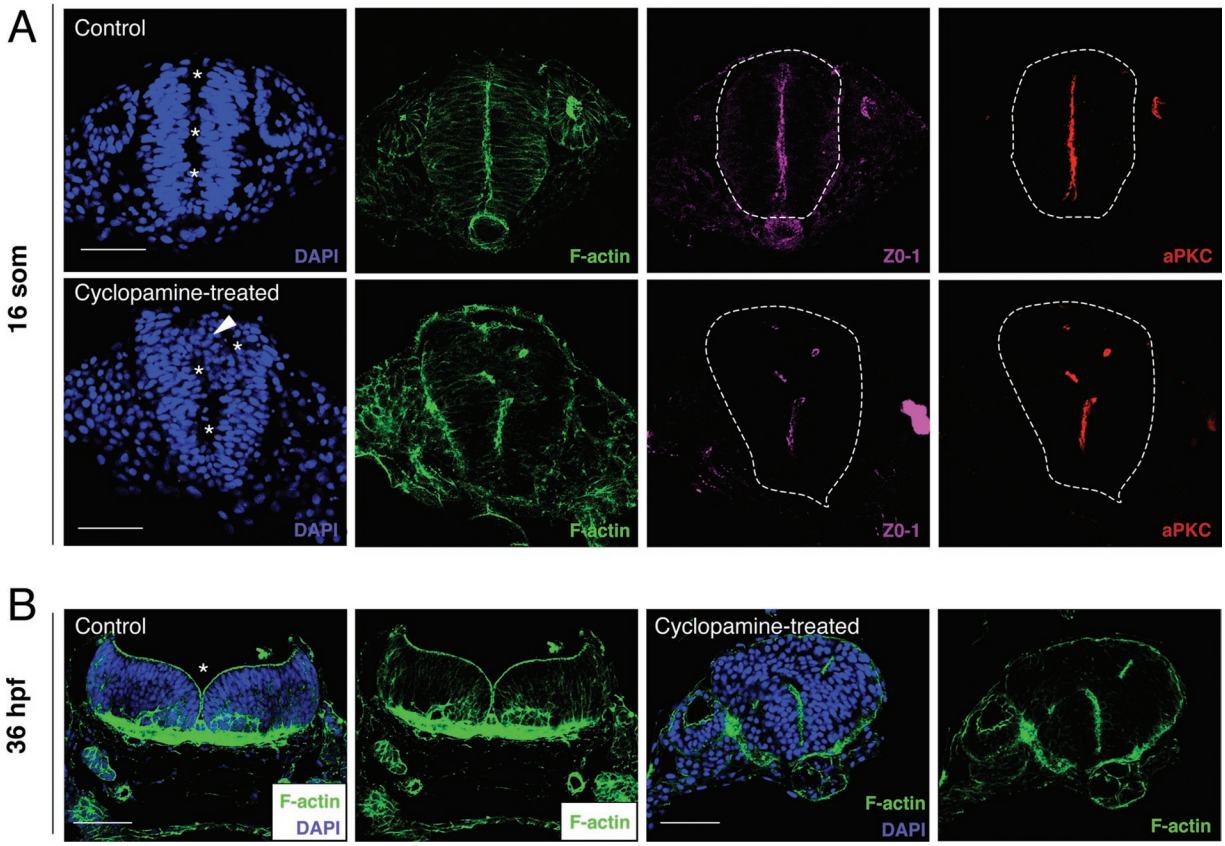

FIGURE 8: Hh signaling regulates apicobasal polarity. (A) Control and cyclopamine-treated embryos at 16 som labeled with phalloidin (F-actin, green), ZO-1 (tight junction marker, pink), aPKC (apical marker, red), and DAPI (blue). Asterisks indicate the lumen of the neural tube. White arrowhead indicates cells extruded from the neural tube into the lumen. The neural tube is outlined by a dashed line in the images showing single channels. (B) Control and cyclopamine-treated embryos at 36 hpf labeled with phalloidin (green) and DAPI (blue). Scale bar = 20 μm.

controls neural progenitor proliferation (Jeong and McMahon, 2005; Cayuso *et al.*, 2006; Alvarez-Medina *et al.*, 2009). Although Hh protein forms a gradient in the neural tube that is highest in ventral regions, Hh signaling is apparently required throughout the entire dorsoventral axis of the chick neural tube to regulate cell-cycle progression (Alvarez-Medina *et al.*, 2009). In this regard, Shh has been shown to function upstream of Wnt signaling to promote *cyclin-D1* expression and the G1/S transition. Shh also controls G2 length by regulating the expression of late cyclins independently of the Wnt pathway (Alvarez-Medina *et al.*, 2009). The finding that hyperproliferation in *N-cad* mutants is mediated by ectopic Hh signaling is consistent with the well-documented promitotic activity of Hh signaling. Our data, however, suggest that this pathway is required for cell-cycle progression only at later stages of zebrafish neural tube development. Indeed, cyclopamine treatment does not alter mitotic indices in 16 som embryos but does cause a dramatic reduction in the size of the neural tube at 36 hpf. Taken together, these observations suggest a biphasic requirement for Hh signaling in zebrafish, to specify ventral cell fates in the early neural tube (Ericson *et al.*, 1997), and to promote cell proliferation at later stages of neural development. Early dorsal progenitors in the zebrafish are apparently responsive to Hh signaling and undergo hyperproliferation when this pathway is abnormally activated in *N-cad* mutants.

Hh signaling has been shown to promote integrin-based adhesion in the neural tube (Fournier-Thibault *et al.*, 2009). We provide evidence here that this pathway also controls cell–cell adhesion, through apical junction assembly (including AJs) in the dorsal neural tube. Thus, there appears to be a reciprocal interaction between AJs and Hh signaling. This feedback loop reveals a putative mechanism by which Hh signaling may limit the range of its own activity. The fact that cell polarization is only disrupted in dorsal regions of cyclopamine-treated embryos suggests that Hh interacts with a spatially restricted signal controlling junctional complex assembly. Together these findings provide several new perspectives on N-cad function in maintaining homeostasis in the neural tube.

MATERIALS AND METHODS

Zebrafish strains and embryo staging

All WT analyses were performed using the AB or TL strain (the latter was used for MO injections). *N-cad*^{p79emcf} mutants were obtained from M. Granato (Department of Cell and Developmental Biology, University of Pennsylvania), *N-cad*$^{R2.10}$ from W. Köster, and HuC-Kaede (Sato *et al.*, 2006) from H. Okamoto (RIKEN, Brain Science Institute). *Ncad*^{p79emcf} is a missense mutation, resulting in a change from an isoleucine to serine at position 676 in the EC5 domain and is thought to be semidominant (Birely *et al.*, 2005). *N-cad*$^{R2.10}$ is a null allele due to incorrect splicing (Lele *et al.*, 2002). Embryos were collected at stages ranging from shield to 48 hpf (Kimmel *et al.*, 1995).

Microinjections

MOs were generated against the translation initiation start site of zebrafish *gli1, gli2a, N-cad, shh,* and *twhh* with the following

sequences: *gli1* MO: 5′CCGACACACCCGCTACACCCACAGT 3′ (Karlstrom *et al.*, 2003); *gli2a* MO: 5′ GGATGATGTAAAGTTCGTCAGTTGC 3′ (Karlstrom *et al.*, 2003); *N-cad* MO: 5′TCTGTATAAAGAAACCGATAGAGTT-3′ (Lele *et al.*, 2002); *shh-2*-MO: 5′-TGTCTAGCAGGGTTTCTC GTTGTCG- 3′ (Ekker and Larson, 2001); and *twhh* MO: 5′TTCCATGACGTTTGAATTATCTCTT-3′ (Nasevicius and Ekker, 2000).

The specificity of all of these MOs has been previously tested, and we confirm here the morphological phenotypes associated with the loss of function of these genes (Nasevicius and Ekker, 2000; Ekker and Larson, 2001; Lele *et al.*, 2002; Karlstrom *et al.*, 2003).

shh mRNA for injection was synthesized by linearizing *shh* plasmid (obtained from J. Du, Center of Marine Biotechnology, University of Maryland) with *Bam*H1 and transcribing with T7 polymerase using mMESSAGE mMACHINE (Ambion. Austin, TX).

N-cad MO was injected at a concentration of 1 mg/ml; *gli1*, *gli2*, *shh,* and *twhh* MOs were injected at 2 mg/ml; and capped *shh* mRNA was injected at a concentration of 820 mg/ml.

EGTA treatment

Twenty som embryos were dechorionated and incubated with 20 mM EGTA in embryo medium for 30 min, washed three times in embryo medium without shaking, and fixed in 4% paraformaldehyde (PFA). The duration of the treatment was deliberately short to avoid extensive tissue damage.

Cyclopamine treatment

To disrupt Hh signaling, embryos were treated with cyclopamine (Lot No. BAC-116; LC Laboratories,Woburn, MA), a plant-derived alkaloid shown to block cellular response to Hh signaling (Chen *et al.*, 2002). Embryos were incubated in 150 µM cyclopamine with 1% ethyl alcohol (ETOH) beginning at the shield stage and fixed either at 16 som or 36 hpf. Control embryos were treated with 1% ETOH.

Embryos treated with cyclopamine exhibit partial cyclopia (a hallmark of reduced Shh signaling) and U-shaped somites. To verify the effectiveness of the treatment, embryos were labeled with a riboprobe for *ptc1*, a target of the Hh pathway. Our results indicate that embryos treated with cyclopamine have diminished expression of *ptc1* (unpublished data), suggesting that the treatment is effective in abolishing Hh signaling.

Labeling and imaging of fixed preparations

Wholemount in situ hybridization was performed as described (Thisse *et al.*, 1993). To synthesize antisense digoxigenin RNA probes, *gli1* and *gli2a* were linearized with *Bam*H1 and transcribed with T7 polymerase, *ptc1* was linearized with *Xba*I and transcribed with T3 polymerase, and *shh* was linearized with *Hind*III and transcribed with T7 polymerase.

Immunolabeling was done on floating sections or wholemounts, according to the Westerfield protocol (Westerfield, 2000), with the modification that embryos to be labeled with anti-HuC antibody were boiled in 50 mM Tris, pH 8.0, for 30 min for antigen retrieval and were permeabilized in 0.2% phosphate-buffered saline Tween-20 for 30 min prior to immunolabeling.

Antibodies used on floating sections were as follows: mouse anti-β-catenin (BD Biosciences) at 1:200, rabbit-anti-aPKCζ (Santa Cruz Biotechnology, Santa Cruz, CA) at 1:200, mouse anti-ZO-1 (Zymed Laboratories, South San Francisco, CA) at 1:200, mouse-anti-Ace-Tub (Sigma, St. Louis, MO) at 1:200, and mouse-anti-γ-tubulin (Sigma) at 1:200. The following antibodies were used on whole mounts: mouse anti-HuC/HuD (Invitrogen, Carlsbad, CA) at 20 µg/ml, rabbit anti-Sox3C (a gift from M. Klymkowsky, Molecular, Cellular and Developmental Biology, University of Colorado, Boulder) at 1:1000, mouse anti-PH3 (Upstate Biotechnology, Lake Placid, NY) at 1:200, rabbit anti-PH3 (Upstate Biotechnology) at 1:200, and mouse anti-BrdU conjugated to Alexa-594 (Molecular Probes, Eugene, OR) at 1:200. Secondary antibodies conjugated to Alexa-488 or Cy3 (Molecular Probes) were used at 1:200. Phalloidin-Alexa-488 (Molecular Probes) was used at 1:75. DAPI (4′,6-diamidino-2-phenylindole; Molecular Probes) was used according to the manufacturer's instructions.

Sectioning was performed on fixed embryos that were mounted in 4% low-melting-point agarose (Shelton Scientific, IBI, Shelton, CT) and cut with a thickness of 40 µm using a vibratome (1500 Sectioning System; Vibratome 1500, St. Louis, MO). Sections through the hindbrain region were selected based on the presence of otic vesicles. Labeled sections were imaged with a Zeiss (Thornwood, NY) LSM 510 META or a Leica (Buffalo Grove, IL) SP5 confocal microscope by collecting 1-µm-thick Z-stacks. Sectioned embryos processed for in situ hybridization were imaged using a Zeiss Axioskop.

Analysis of cell-cycle exit

Cell-cycle exit was analyzed by dechorionating 12 som WT embryos and *N-cad*^{p79emcf} mutants and exposing them to 10 mM BrdU (Sigma) in embryo medium with 15% dimethyl sulfoxide on ice for 20 min. Embryos were then washed 10 times in embryo medium, staged to 36 hpf, and fixed in 4% PFA (for anti-BrdU and anti-Sox3C) or Prefer fix (Anatech, Battle Creek, MI) (for anti-BrdU and anti-HuC). Following fixation, embryos were immunolabeled with anti-BrdU and anti-Sox3C or anti-HuC, sectioned, and imaged. Despite the presence of mitotic neurons in *N-cad* mutants that are HuC-positive, the use of this marker for cell-cycle exit and differentiation is justifiable because these cells represent a negligible fraction of the total number of mitotic cells.

Analysis of cell-cycle length

Analysis of cell-cycle length was performed on dechorionated 8 som,14 som, and 16 som WT and *N-cad*^{p79emcf} embryos that were exposed to 10 mM BrdU for 20 min on ice. The embryos were then fixed in 4% PFA, labeled with anti-BrdU and anti-Sox3C, sectioned, and imaged.

Quantification and statistical analysis

All quantifications were performed using Z stacks through 40-µm-thick hindbrain sections. Cells were counted using the Zeiss LSM or Leica LAS software and a manual counter, unless otherwise indicated.

Mitotic indices. Mitotic indices were scored in the hindbrain regions using embryos labeled with anti-Sox3C and anti-PH3. Mitotic indices in WT and *N-cad* mutants were scored using three embryos (three sections per embryo) at 8 som, 30 hpf, and 42 hpf, and six embryos (three sections per embryo) at 12 som and 16 som. Mitotic indices for rescue attempts with cyclopamine, *shh/twhh* or *gli1* and *gli2* MO injections and following *shh* mRNA injections were scored using five embryos (three sections per embryo) and four embryos (three sections per embryo) for controls. The mitotic index was calculated by dividing the total number of mitotic cells (PH3-positive) by the total number of progenitor cells (Sox3C-positive) in the section or by the total number of DAPI-positive cells (for the *shh* overexpression experiment specifically).

Total cell count. Total cell counts were done in DAPI-labeled embryos (three embryos, three sections per embryo) at

developmental stages ranging from 8 som to 60 hpf. A total of four frames per Z-stack were scored using Image J software.

Cell-cycle exit. The ratios of BrdU- and HuC-positive cells or BrdU-positive and Sox3C-negative cells to the total number of BrdU-positive cells in 40-μm-thick sections were quantified to evaluate cell-cycle exit rates in WT versus *N-cad* mutants. The larger the ratio, the faster the withdrawal from the cell cycle.

Cell-cycle length. The ratios of BrdU- and Sox3C-positive cells over the total number of Sox3C-positive cells in 40-μm-thick sections were quantified to estimate cell-cycle lengths in WT versus *N-cad* mutants. The larger the ratio, the longer the cell cycle is predicted to be.

Mitotic neurons. Mitotic neurons were scored in HuC-Kaede transgenic embryos that were labeled with anti-PH3. The total numbers of double-positive cells were counted in six embryos (three sections per embryo) at 24 hpf, three embryos (three sections per embryo) in *N-cad* MO-injected embryos at 48 hpf, and 15 embryos (three sections per embryo) at 48 hpf in *N-cad*^{p79emcf} mutants. Mitotic neurons were also scored in embryos immunolabeled with anti-HuC and anti-PH3 at 48 hpf (five embryos, three sections per embryo).

Quantifications from different sections obtained from the same embryo were added to obtain total numbers per embryo. These values were used to determine the average, SD, and SE per genotype. The p value for statistical significance was obtained by logistic regression analysis using the SAS system (SAS Institute, Cary, NC)for mitotic indices; the Student's *t* test for total cell counts, cyclopamine treatment, cell-cycle exit, and cell-cycle length studies; and a contingency table for mitotic HuC-positive cells.

ACKNOWLEDGMENTS

We thank Sreekanth Chalasani, Chen-Ming Fan, and Mark Van Doren for their comments and suggestions; Jeff Leips for help with statistical analyses; Chere Petty for assistance with confocal imaging; and Michael Klymkowsky for his generous gift of anti-Sox3C. This work was supported by a grant from the National Institute of General Medical Sciences (NIGMS; 1R01GM085290–01A1). The Leica SP5 confocal microscope was purchased with funds from the National Science Foundation (DBI-0722569).

REFERENCES

Alvarez-Medina R, Le Dreau G, Ros M, Marti E (2009). Hedgehog activation is required upstream of Wnt signalling to control neural progenitor proliferation. Development (Cambridge, England) 136, 3301–3309.

Benjamin JM, Kwiatkowski AV, Yang C, Korobova F, Pokutta S, Svitkina T, Weis WI, Nelson WJ (2010). AlphaE-catenin regulates actin dynamics independently of cadherin-mediated cell-cell adhesion. J Cell Biol. 189, 339–352.

Benjamin JM, Nelson WJ (2008). Bench to bedside and back again: molecular mechanisms of alpha-catenin function and roles in tumorigenesis. Semin Cancer Biol 18, 53–64.

Birely J, Schneider VA, Santana E, Dosch R, Wagner DS, Mullins MC, Granato M (2005). Genetic screens for genes controlling motor nerve-muscle development and interactions. Dev Biol 280, 162–176.

Buttitta LA, Edgar BA (2007). Mechanisms controlling cell cycle exit upon terminal differentiation. Curr Opin Cell Biol 19, 697–704.

Buttitta LA, Katzaroff AJ, Edgar BA (2010). A robust cell cycle control mechanism limits E2F-induced proliferation of terminally differentiated cells in vivo. J Cell Biol 189, 981–996.

Buttitta LA, Katzaroff AJ, Perez CL, de la Cruz A, Edgar BA (2007). A double-assurance mechanism controls cell cycle exit upon terminal differentiation in Drosophila. Dev Cell 12, 631–643.

Caspary T, Larkins CE, Anderson KV (2007). The graded response to Sonic Hedgehog depends on cilia architecture. Dev Cell 12, 767–778.

Cayuso J, Ulloa F, Cox B, Briscoe J, Marti E (2006). The Sonic hedgehog pathway independently controls the patterning, proliferation and survival of neuroepithelial cells by regulating Gli activity. Development (Cambridge, England) 133, 517–528.

Chalasani K, Brewster R (2010). Loss of cell adhesion disrupts the organization of the neural tube. Mol Reprod Dev 77, 1.

Chen D, Opavsky R, Pacal M, Tanimoto N, Wenzel P, Seeliger MW, Leone G, Bremner R (2007). Rb-mediated neuronal differentiation through cell-cycle-independent regulation of E2f3a. PLoS Biol 5, e179.

Chen JK, Taipale J, Cooper MK, Beachy PA (2002). Inhibition of Hedgehog signaling by direct binding of cyclopamine to Smoothened. Genes Dev 16, 2743–2748.

Chen Y, Struhl G (1996). Dual roles for patched in sequestering and transducing Hedgehog. Cell 87, 553–563.

Chenn A, Walsh CA (2002). Regulation of cerebral cortical size by control of cell cycle exit in neural precursors. Science 297, 365–369.

Clevers H (2006). Wnt/beta-catenin signaling in development and disease. Cell 127, 469–480.

Eggenschwiler JT, Anderson KV (2007). Cilia and developmental signaling. Annu Rev Cell Dev Biol 23, 345–373.

Ekker SC, Larson JD (2001). Morphant technology in model developmental systems. Genesis 30, 89–93.

Ericson J, Briscoe J, Rashbass P, van Heyningen V, Jessell TM (1997). Graded sonic hedgehog signaling and the specification of cell fate in the ventral neural tube. Cold Spring Harb Symp Quant Biol 62, 451–466.

Firth LC, Baker NE (2005). Extracellular signals responsible for spatially regulated proliferation in the differentiating Drosophila eye. Dev Cell 8, 541–551.

Fournier-Thibault C, Blavet C, Jarov A, Bajanca F, Thorsteinsdottir S, Duband JL (2009). Sonic hedgehog regulates integrin activity, cadherin contacts, and cell polarity to orchestrate neural tube morphogenesis. J Neurosci 29, 12506–12520.

Geldmacher-Voss B, Reugels AM, Pauls S, Campos-Ortega JA (2003). A 90-degree rotation of the mitotic spindle changes the orientation of mitoses of zebrafish neuroepithelial cells. Development (Cambridge, England) 130, 3767–3780.

Grigoryan T, Wend P, Klaus A, Birchmeier W (2008). Deciphering the function of canonical Wnt signals in development and disease: conditional loss- and gain-of-function mutations of beta-catenin in mice. Genes Dev 22, 2308–2341.

Harrington MJ, Hong E, Fasanmi O, Brewster R (2007). Cadherin-mediated adhesion regulates posterior body formation. BMC Dev Biol 7, 130.

Hatta K, Takeichi M (1986). Expression of N-cadherin adhesion molecules associated with early morphogenetic events in chick development. Nature 320, 447–449.

Hong E, Brewster R (2006). N-cadherin is required for the polarized cell behaviors that drive neurulation in the zebrafish. Development (Cambridge, England) 133, 3895–3905.

Huang P, Schier AF (2009). Dampened Hedgehog signaling but normal Wnt signaling in zebrafish without cilia. Development (Cambridge, England) 136, 3089–3098.

Jarov A, Williams KP, Ling LE, Koteliansky VE, Duband JL, Fournier-Thibault C (2003). A dual role for Sonic hedgehog in regulating adhesion and differentiation of neuroepithelial cells. Dev Biol 261, 520–536.

Jeanes A, Gottardi CJ, Yap AS (2008). Cadherins and cancer: how does cadherin dysfunction promote tumor progression? Oncogene 27, 6920–6929.

Jeong J, McMahon AP (2005). Growth and pattern of the mammalian neural tube are governed by partially overlapping feedback activities of the hedgehog antagonists patched 1 and Hhip1. Development (Cambridge, England) 132, 143–154.

Kadowaki M, Nakamura S, Machon O, Krauss S, Radice GL, Takeichi M (2007). N-cadherin mediates cortical organization in the mouse brain. Dev Biol 304, 22–33.

Karlstrom RO, Tyurina OV, Kawakami A, Nishioka N, Talbot WS, Sasaki H, Schier AF (2003). Genetic analysis of zebrafish gli1 and gli2 reveals divergent requirements for gli genes in vertebrate development. Development (Cambridge, England) 130, 1549–1564.

Kim HR, Richardson J, van Eeden F, Ingham PW (2010). Gli2a protein localization reveals a role for Iguana/DZIP1 in primary ciliogenesis and a dependence of Hedgehog signal transduction on primary cilia in the zebrafish. BMC Biol 8, 65.

Kimmel CB, Ballard WW, Kimmel SR, Ullmann B, Schilling TF (1995). Stages of embryonic development of the zebrafish. Dev Dyn 203, 253–310.
Kobielak A, Fuchs E (2006). Links between alpha-catenin, NF-kappaB, and squamous cell carcinoma in skin. Proc Natl Acad Sci USA 103, 2322–2327.
Lee J, Platt KA, Censullo P, Ruiz i Altaba A (1997). Gli1 is a target of Sonic hedgehog that induces ventral neural tube development. Development (Cambridge, England) 124, 2537–2552.
Lele Z, Folchert A, Concha M, Rauch GJ, Geisler R, Rosa F, Wilson SW, Hammerschmidt M, Bally-Cuif L (2002). Parachute/n-cadherin is required for morphogenesis and maintained integrity of the zebrafish neural tube. Development (Cambridge, England) 129, 3281–3294.
Lien WH, Gelfand VI, Vasioukhin V (2008a). Alpha-E-catenin binds to dynamitin and regulates dynactin-mediated intracellular traffic. J Cell Biol 183, 989–997.
Lien WH, Klezovitch O, Fernandez TE, Delrow J, Vasioukhin V (2006). AlphaE-catenin controls cerebral cortical size by regulating the hedgehog signaling pathway. Science 311, 1609–1612.
Lien WH, Stepniak E, Vasioukhin V (2008b). Dissecting the role of cadherin-catenin proteins in mammalian epidermis. Proc Natl Acad Sci USA 105, 15225–15226.
Locker M, Agathocleous M, Amato MA, Parain K, Harris WA, Perron M (2006). Hedgehog signaling and the retina: insights into the mechanisms controlling the proliferative properties of neural precursors. Genes Dev 20, 3036–3048.
Lyons DA, Guy AT, Clarke JD (2003). Monitoring neural progenitor fate through multiple rounds of division in an intact vertebrate brain. Development (Cambridge, England) 130, 3427–3436.
Machon O, Van Den Bout CJ, Backman M, Kemler R, Krauss S (2003). Role of beta-catenin in the developing cortical and hippocampal neuroepithelium. Neurosci 122, 129–143.
Megason SG, McMahon AP (2002). A mitogen gradient of dorsal midline Wnts organizes growth in the CNS. Development (Cambridge, England) 129, 2087–2098.
Munson C, Huisken J, Bit-Avragim N, Kuo T, Dong PD, Ober EA, Verkade H, Abdelilah-Seyfried S, Stainier DY (2008). Regulation of neurocoel morphogenesis by Pard6 gamma b. Dev Biol 324, 41–54.
Nasevicius A, Ekker SC (2000). Effective targeted gene "knockdown" in zebrafish. Nature Genet 26, 216–220.
Nelson WJ (2008). Regulation of cell-cell adhesion by the cadherin-catenin complex. Biochem Soc Trans 36, 149–155.
Niessen CM, Gottardi CJ (2008). Molecular components of the adherens junction. Biochim Biophys Acta 1778, 562–571.
Panhuysen M, Vogt Weisenhorn DM, Blanquet V, Brodski C, Heinzmann U, Beisker W, Wurst W (2004). Effects of Wnt1 signaling on proliferation in the developing mid-hindbrain region. Mol Cell Neurosci 26, 101–111.
Pascale A, Amadio M, Quattrone A (2008). Defining a neuron: neuronal ELAV proteins. Cell Mol Life Sci 65, 128–140.
Perrais M, Chen X, Perez-Moreno M, Gumbiner BM (2007). E-cadherin homophilic ligation inhibits cell growth and epidermal growth factor receptor signaling independently of other cell interactions. Mol Biol Cell 18, 2013–2025.
Radice GL, Rayburn H, Matsunami H, Knudsen KA, Takeichi M, Hynes RO (1997). Developmental defects in mouse embryos lacking N-cadherin. Dev Biol 181, 64–78.
Sage C *et al*. (2005). Proliferation of functional hair cells in vivo in the absence of the retinoblastoma protein. Science 307, 1114–1118.
Sato T, Takahoko M, Okamoto H (2006). HuC:Kaede, a useful tool to label neural morphologies in networks in vivo. Genesis 44, 136–142.
Scott JA, Yap AS (2006). Cinderella no longer: alpha-catenin steps out of cadherin's shadow. J Cell Sci 119, 4599–4605.
Sellers WR, Novitch BG, Miyake S, Heith A, Otterson GA, Kaye FJ, Lassar AB, Kaelin WG, Jr (1998). Stable binding to E2F is not required for the retinoblastoma protein to activate transcription, promote differentiation, and suppress tumor cell growth. Genes Dev 12, 95–106.
Shtutman M, Zhurinsky J, Simcha I, Albanese C, D'Amico M, Pestell R, Ben-Ze'ev A (1999). The cyclin D1 gene is a target of the beta-catenin/LEF-1 pathway. Proc Natl Acad Sci USA 96, 5522–5527.
Teng J, Rai T, Tanaka Y, Takei Y, Nakata T, Hirasawa M, Kulkarni AB, Hirokawa N (2005). The KIF3 motor transports N-cadherin and organizes the developing neuroepithelium. Nat Cell Biol 7, 474–482.
Thisse C, Thisse B, Schilling TF, Postlethwait JH (1993). Structure of the zebrafish snail1 gene and its expression in wild-type, spadetail and no tail mutant embryos. Development (Cambridge, England) 119, 1203–1215.
Tinkle CL, Pasolli HA, Stokes N, Fuchs E (2008). New insights into cadherin function in epidermal sheet formation and maintenance of tissue integrity. Proc Natl Acad Sci USA 105, 15405–15410.
Tissir F *et al*. (2010). Lack of cadherins Celsr2 and Celsr3 impairs ependymal ciliogenesis, leading to fatal hydrocephalus. Nat Neurosci 13, 700–707.
Vasioukhin V (2006). Lethal giant puzzle of Lgl. Dev Neurosci 28, 13–24.
Vasioukhin V, Bauer C, Degenstein L, Wise B, Fuchs E (2001). Hyperproliferation and defects in epithelial polarity upon conditional ablation of alpha-catenin in skin. Cell 104, 605–617.
Westerfield M (2000). The Zebrafish Book. A Guide for the Laboratory Use of Zebrafish (Danio rerio), 4th ed., Eugene, OR: University of Oregon Press.
Wilson CW, Stainier DY (2010). Vertebrate Hedgehog signaling: cilia rule. BMC Biol 8, 102.
Zechner D, Fujita Y, Hulsken J, Muller T, Walther I, Taketo MM, Crenshaw EB, 3rd, Birchmeier W, Birchmeier C (2003). beta-Catenin signals regulate cell growth and the balance between progenitor cell expansion and differentiation in the nervous system. Dev Biol 258, 406–418.